Boundary-Layer Meteorol (2010) 137:291–305
DOI 10.1007/s10546-010-9533-9

ARTICLE

Evaluating the Effects of Radiative Forcing Feedback in Modelling Urban Ozone Air Quality in Portland, Oregon: Two-Way Coupled MM5–CMAQ Numerical Model Simulations

Haider Taha · David Sailor

Received: 15 October 2009 / Accepted: 28 July 2010 / Published online: 27 August 2010

Abstract We summarize an on-line coupled meteorological–emissions–photochemical modelling system that allows feedback from air-quality/chemistry to meteorology via radiative forcing. We focus on the radiative-forcing impacts (direct effects) of ozone. We present an application of the coupled modelling system to the episode of 23–31 July 1998 in Portland, Oregon, U.S.A. Results suggest that the inclusion of radiative-forcing feedback produces small but accountable impacts. For this region and episode, stand-alone radiative transfer simulations, i.e., evaluating the effects of radiative forcing independently of changes in meteorology or emissions, suggest that a change of 1 ppb in ground-level ozone is approximately equivalent to a change of 0.017 W m^{-2} in radiative forcing. In on-line, coupled, three-dimensional simulations, where the meteorological dependencies are accounted for, domain-wide peak ozone concentrations were higher by 2–4 ppb (relative to a simulated peak of 119.4 ppb) when including the effects of radiative-forcing feedback. A scenario of 10% reduction in anthropogenic emissions produced slightly larger decreases in ozone, an additional 1 ppb in local-peak reductions, relative to scenarios without feedback.

Keywords Air quality · Meteorological numerical modelling · On-line coupling · Photochemical modelling · Radiative forcing

1 Background and Study Goal

We can depict in abstract terms (relations 1 and 2) the meteorology-to-chemistry and chemistry-to-meteorology feedbacks of interest in this study and their implications (listed above the brackets) in meteorological and air-quality modelling, viz.

H. Taha (✉)
Altostratus Inc., 940 Toulouse Way, Martinez, CA 94553, USA
e-mail: haider@altostratus.com
URL: www.altostratus.com

D. Sailor
Mechanical and Materials Engineering Department, Portland State University, Portland, OR 97207, USA

$$met \Rightarrow AQ \in \overbrace{(u, v, w)}^{\text{adv./transp.}}; \overbrace{(K_V, K_H)}^{\text{turb.diff.}}; \overbrace{(R_{\text{actinic}})}^{\text{chem.}}; \overbrace{(Z_i)}^{\text{mix.hgt.}}; \overbrace{(\rho, H_2O)}^{\text{chem.}} \quad (1)$$

$$AQ \Rightarrow met \in \overbrace{(RF)}^{\partial T/\partial t}; \overbrace{(R_{\text{surface}})}^{\partial T_s/\partial t}; \overbrace{(\rho)}^{\text{buoy.TKE}} \quad (2)$$

where, u, v, w are the wind velocity components, K_V and K_H are the vertical and horizontal diffusivities, R is solar radiation, Z_i is mixing height, ρ is density, and RF is radiative forcing. While all aspects of the forward relation (1) have been accounted for and are well represented in conventional meteorological-photochemical modelling frameworks, the feedback relation (2) has been relatively less evaluated and quantified. In particular, quantifying the feedback effects of the first term in relation (2), radiative forcing, is of interest. It should be noted that state-of-science meteorological models, e.g., MM5 (Penn State/NCAR Fifth Generation Mesoscale Model) and WRF (Weather Research and Forecasting model), do incorporate the effects of trace gases (e.g., ozone, O_3) on radiative forcing in internal calculations, but their concentrations are typically taken from prescribed profiles that remain unchanged (during model integration) in response to perturbations in meteorology, emissions, and chemistry.

The current state of air-quality modelling is based mostly on configurations whereby chemistry-transport/photochemical models are driven by meteorological models (off-line) including emission corrections to reflect the effects of changes in the meteorology (Taha 2008a,b). While feedback from photochemical models to meteorological models has not been fully implemented in modelling frameworks typically used in the U.S., significant efforts in this direction have been underway, e.g., Pleim et al. (2008). In Europe, such model linkages have been tested recently, e.g., Baklanov and Korsholm (2007) and Baklanov et al. (2008). Other modelling frameworks, such as the on-line chemistry versions of MM5 (Grell et al. 2000) and WRF also aim at establishing some feedback; however, except for aerosol/cloud radiative effects, they account mostly for one direction of interaction (meteorology affecting air quality—relation (1) above).

The focus of our effort was to develop an on-line coupled system, based on existing models, and which includes feedback capabilities to account for the effects of changing air-pollutant concentrations during model integration. Here, we focus only on the radiative-forcing effects of O_3 (direct effects), and the effects of changes in atmospheric aerosol loading, both direct and indirect, are not accounted for. In the simulations presented here, aerosols are given by either urban or background tropospheric profiles, depending on the location in the domain. Evaluating the effects of changes in aerosol loading and other trace-gas concentrations on radiative forcing and meteorology is planned for the near future.[1]

[1] In terms of radiative forcing (greenhouse efficiency), methane (CH_4) and ozone (O_3) both have significant impacts and the effects of O_3 are more significant than those of its precursors (non-methane organics, NMOC, and oxides of nitrogen, NO_x). In this paper we assume no changes in CH_4 as a result of localized and episodic emission control and, because O_3 has a relatively larger radiative forcing than its precursors, we also ignore their effects at this time. The coupled modelling system we discuss here, however, will allow us to study variations in these and other species. The assumptions we make here may be justified because changes in NO_x, NMOC, and carbon monoxide (CO) emissions impart net radiative forcing mainly because of the resulting changes in tropospheric O_3 and CH_4, while changes in NO_x alone do not impart an effect on radiative forcing (Naik et al. 2005). Of course, there are other greenhouse gases to consider, including carbon dioxide (CO_2), water vapour (H_2O), nitrous oxide (N_2O), chlorofluorocarbons (CFCs), and aerosols but, as discussed herein, we assume that their concentrations do not change significantly at the urban and temporal scales (episodic conditions) considered and simulated here.

2 Approach

Our approach in the on-line coupling of meteorological, emissions, chemistry transport–photochemical and radiative-transfer models is termed "on-line access" in WMO (2008) and includes model interfaces where needed. In on-line access, data from any of these models are available for use by another at each timestep or multiple timesteps. Section 2.1 presents the models and the configurations we used,while the specifics of implementing the on-line access coupling in this study are discussed in Sect. 2.2.

2.1 Models

2.1.1 Meteorology

We used an in-house modified version of the MM5, based on release 3.6 of the model (see Dudhia 1993; Grell et al. 1994) so as to incorporate more resolved urban land-use and land-cover (LULC) categories in addition to the LULC that the standard model recognizes (Fan and Sailor 2005). The use of more resolved urban LULC and urban canopy parameterizations (Taha 2008a) introduces greater spatial detail in thermophysical properties, e.g., albedo, emissivity, roughness length, thermal inertia, and soil moisture content, as well as in urban geometrical properties. Updated and more resolved LULC are also important for improving the radiative-transfer calculations, as discussed in Sect. 2.1.3. In addition, the MM5 was modified to incorporate land-use-dependent profiles of anthropogenic heat flux (Fan and Sailor 2005). For this study, the model was run with the standard 24 U.S. Geological Survey (USGS) LULC categories plus an additional six urban LULC. On the stand-alone 4- km grid discussed in Sect. 2.5, the model was run without four-dimensional data assimilation, using a 5-layer soil model, and a boundary-layer scheme (Gayno-Seaman) that predicts turbulent kinetic energy (TKE) (Janjic and Zavisa 1994).

2.1.2 Chemistry-Transport/Photochemistry

We used the Models-3/Community Multiscale Air Quality model (CMAQ CTM) (Byun and Schere 2006) for photochemical modelling. CMAQ was used to establish the baseline conditions of, and to simulate the changes in, tropospheric/urban O_3 as a result of emissions control in the Portland domain. In this study, the model was configured to run with the SAPRC-99 chemical mechanism, was initialized with observational data from 23 July 1998, and run from 23 to 29 July.

2.1.3 Radiative Transfer

For radiative-transfer calculations in our coupled modelling system, *Streamer* (Key and Schweiger 1998; Key 2001) was integrated as an intermediate module that provides feedback, i.e., heating/cooling rates, from CMAQ to MM5. For a detailed discussion of the science and formulations in the *Streamer* radiative-transfer model (RTM) of Key (2001), see Brieglieb et al. (1986), Stamnes et al. (1988), Toon et al. (1989), Tsay et al. (1989), Ebert and Curry (1992), Hu and Stamnes (1993) and Kylling et al. (1995). The model is also fully discussed in Key (2001); here we list only some of the highlights.

Streamer is comparable to LOWTRAN/MODTRAN (Snell et al. 1995) and its performance is similar to or better than other radiative-transfer models available in the public domain, e.g., CCM2/CCM3, and RRTM (Pinto et al. 1997). Flux computations can be done

using two or more streams and the model calculates upwelling and downwelling shortwave and longwave radiation, net fluxes, cloud radiative effects, and heating/cooling rates, considering various surface properties, LULC, albedo, and emissivity. The model uses 24 shortwave and 105 longwave computational bands. Gases considered are O_3, CO_2, O_2, and H_2O. Precursors of O_3, e.g., NO_x and volatile organic compounds are not explicitly represented, which may overestimate the radiative-forcing effects of O_3 simulated with this model.

The RTM includes a solver for a two-stream method as well as a discrete ordinate solver (Key 2001). The two-stream method (Toon et al. 1989) was used in this study with gas absorption data from Tsay et al. (1989). In this application, the computed shortwave and longwave radiative fluxes using the two-stream method were within 5% of those computed with multiple streams, but the simulations were much faster. Optical properties for water clouds are parameterized based on Hu and Stamnes (1993), Schmidt et al. (1995) and Takano and Liou (1989). Optical properties for ice clouds are parameterized according to Fu and Liou (1993). As with other RTMs, cloud parameterizations in *Streamer* account for water content, extinction, particle radii, single scattering albedo, and the asymmetry parameter. The radiative effects of aerosols are parameterized via their extinction-coefficient profiles, whether idealized or specified. The model has several built-in vertical profiles of scaling factors (representing various atmospheric loading situations) that can be used in conjunction with several extinction-coefficient spectral profiles. In this study, an urban aerosol model was used in conjunction with a background tropospheric scaling profile. Gas absorption is parameterized using an exponential sum-fitting technique and the data are based on Tsay et al. (1989). This technique approximates the spectrally-integrated fluxes via a number of weighted exponential terms. Heating and cooling rates between any two atmospheric levels (e.g., levels in the meteorological model) are computed based on flux divergence and pressure difference.

In our coupled modelling system, the RTM requires time-dependent gridded input of vertical profiles of pressure, temperature, water vapour mixing ratio, O_3 mixing ratio, and aerosol optical depth. It also requires specification of LULC and dependent surface properties, such as broadband albedo and emissivity at each grid cell (thus the importance of improving LULC characterization). It also requires gridded surface temperature. These gridded vertical profiles and surface properties are passed to the RTM from the meteorological (MM5) and chemistry-transport (CMAQ CTM) models in addition to land-use processing modules, see below.

2.1.4 Emissions

While both anthropogenic and biogenic emissions can be influenced by meteorology (surface and air temperatures, pressure, solar radiation), initially, the priority was to focus on biogenic-emission corrections for implementation in the coupled modelling system. Note that this discussion is provided for the sake of completeness; emission corrections were not actually performed in the Portland domain simulations (discussed in Sect. 2.2).

Biogenic volatile organic compounds (BVOC) emission rates in the coupled modelling system are updated for changes in temperature and photosynthetically-active radiation based on a widely-used environmental correction algorithm by Guenther et al. (1993). The corrections are applied to emissions of several compounds including isoprene, monoterpenes, methylbutenol, and oxygenated volatile organic compounds.

2.2 Model Linkages

In our on-line coupled modelling system, the meteorological model is called first for one timestep (or several timesteps). Once the model is integrated over that interval, relevant

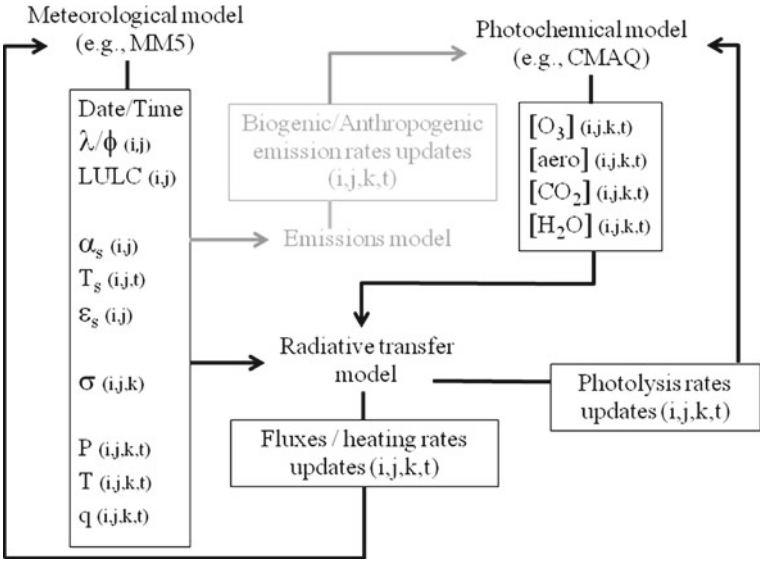

Fig. 1 Timestep loop in the coupled modelling system showing variables and data flow with respect to the radiative-transfer model. The emissions processing module is "dimmed" since it was not active in the present simulations

variables are extracted and passed to the RTM and, if selected, a BVOC emissions correction module. Variables from the meteorological model and from the emissions-correction module are then passed to the CTM. The photochemical model is run for a specified interval and variables are extracted to feed into the RTM along with data from the meteorological model. Finally, the RTM is integrated and, in this application, heating/cooling rates are extracted and passed back to the meteorological model. This loop (part of which is shown in Fig. 1) is then repeated for subsequent timesteps.

Thus, in this system, three types of input are provided to the RTM. The first is meteorological, the second is chemical, and the third relates to surface properties. At each timestep, t, the following variables are provided to the RTM:

- From the meteorological model, 4-dimensional (x, y, z, t) values of air temperature and water-vapour mixing ratio, and 3-dimensional (x, y, t) surface temperature are provided. If a cloud parameterization scheme is used in the meteorological model, then 3-dimensional (x, y, t) cloud-base and cloud-top heights are also provided to the RTM (but this was not used at this application's 4 km grid).
- From the CTM, O_3 mixing ratios are passed to the RTM. As discussed earlier, aerosol loading is assumed unchanged between the base case and perturbation scenarios and is set to background tropospheric values in the non-urban areas of the domain. In the urban areas, aerosol optical depth was assumed constant at a value of 0.04. While such a value is typical for the urban environment, it can be much larger during pollution events (Jin et al. 2005).

Domain-specific, time-independent data are also passed to the RTM including (1) gridded surface albedo, (2) gridded land-cover classes, (3) and gridded surface emissivity, in addition to (4) distribution of pressure and σ levels in the modelling domain. The gridded albedo and emissivity values are land-cover-dependent, which we specify according to the domain's

LULC characterization discussed in Sect. 2.1.1. Other variables are also exchanged among the models, e.g., from the meteorological to photochemical models, such as wind, temperature, moisture, and TKE fields. However, the focus of discussion in *this* section is on the linkages with respect to the RTM. Thus we do not discuss those other variables or model links here.

Figure 1 shows the data flow at each timestep, with respect to the RTM. Acronyms and symbols in the figure are as follows: λ and ϕ are longitude and latitude respectively, LULC is land-use/land-cover, α_s, T_s, and ε_s are respectively surface albedo, temperature, and emissivity, σ, P, T, and q are vertical level, pressure, air temperature, and water vapour mixing ratio. Indices *i, j, k, t*, indicate dimensionality (e.g., gridded 2, 3, or 4-dimensional variables, where i and j are horizontal spatial coordinates, k in the vertical direction, and t is time). Note that, while the linkages to the biogenic/anthropogenic emission-correction modules were actually implemented in this study, emission corrections were not performed in the domain simulations discussed and presented herein (thus the emissions model box in Fig. 1 is "dimmed").

As discussed at the beginning of Sect. 2, our coupling of the models allows for data exchange at each timestep or at multiple timesteps (specified time intervals). In this paper, the MM5 integration timestep at the 4 km grid level (see Sect. 2.5) was 12 s and the CMAQ CTM was called every five MM5 steps. The corresponding wall-clock time of course depends on the computing platform's specifications and the modelled domain's configurations, and so does the additional time needed for data exchange and processing in the on-line coupled modelling system relative to that in an off-line configuration. In this study, the processing time for the 4 km grid, relative to simulations without on-line coupling with the RTM, was more than doubled ($\approx$2.3). This additional time was incurred in (1) data exchange from the meteorological model to the RTM, (2) from the CTM to the RTM, (3) running the RTM in two-stream mode, and (4) exchange of data from RTM to meteorological model.

The coupling of models is realized only at the 4-km grid level—the purpose of the coarser meteorological grids being to provide boundary conditions for running the 4-km grid in stand-alone mode. At this level, all models' grids are similar and no nesting is involved within the coupled system. Using similar grids minimizes potential inadvertent issues of mass/energy consistency that can arise when models of different grid resolutions are coupled.

2.3 Base-Case Scenario

We focus on the episode of 23–31 July 1998 in Portland, Oregon. This episode was characterized by high temperatures and high concentrations of ground-level O_3. Peak air temperatures in Portland during July average 26°C, while actual recorded peak temperatures during this episode reached 38°C on 28 July. Ozone concentrations in the greater Portland area also were higher than usual, over 130 ppb on 26, 27, and 28 July at the Carus monitor, located 27 km to the south of Downtown Portland. Another monitor, located 75 km south of Portland, also had some of the highest concentrations during that episode.

For the base-case scenario, the biogenic and anthropogenic emission inventories used in this study were obtained from the State of Oregon's Department of Environmental Quality (DEQ 1999). A discussion of the region's air quality and emissions can be found at http://www.deq.state.or.us. We simulated the regulatory modelling episode of 23–31 July 1998 for meteorology and 24–29 July for emissions/chemistry. For discussion in this paper, we focus on a day of both relatively high ozone and good model performance, 27 July, as discussed in Sect. 3.2.

2.4 Perturbation Scenario

Initially, two emission perturbation scenarios for the Portland area were developed and considered for modelling in this study. One represented actual levels of emission reductions based on results from local field surveys by Semenza et al. (2008). The surveys quantified the Portland general population's response during "action days" to reduce emissions of ozone precursors (e.g., by carpooling, avoiding barbequing, postponing lawn mowing, etc.). The second represented a hypothetical level of emission reductions achieved if a significant portion of the population curtailed those activities.

Because the survey indicated small overall changes in emissions as a result of human behavior alteration, the first scenario was not simulated in this study. However, the survey also found that subgroups within the population did make substantial changes in their behavior as it relates to energy use and air quality, and could have had significant impacts if a larger number was actually involved. Thus an idealized emission reduction scenario was simulated here to evaluate the effects on air quality. This scenario reduces anthropogenic, area- and mobile-source emissions in the greater Portland-Vancouver urban area by 10% (elevated, point sources such as power plants were unaffected). The simulations were first done without and then with feedback from chemistry to meteorology to quantify the effects of including radiative forcing on O_3 concentrations.

2.5 Modelling Domains

The meteorological modelling domain for the U.S. Pacific north-west consists of four nested grids, D01 through D04, with resolutions of 108, 36, 12, and 4 km respectively, as shown in Fig. 2. The only meteorological grid used in the coupled modelling system is the 4- km grid (D04) with horizontal dimensions of 115×115 grid points and 35 vertical layers (36 full σ levels).

The CTM (CMAQ) modelling domain also has a resolution of 4 km and is slightly smaller than the meteorological domain D04 to allow for a buffer of several grid cells around it. Its horizontal dimensions are 99×99 grid points with 22 layers in the vertical extending up to over 3 km above ground level (a.g.l.). Figure 3 shows the 4- km CTM modelling domain. The inscribed black rectangle is expanded to provide more detail of the greater Portland-Vancouver area, including air-quality monitors of interest as well as a delineation of the urban area (within the white oval) and the emission-control domain (white rectangle).

3 Findings

3.1 Stand-Alone RTM Tests

One-dimensional stand-alone RTM simulations (that is, running the RTM alone, not coupled with other models) were performed to verify the model's functionality and to evaluate its sensitivity to changes in various input parameters. One such test was to evaluate the RTM's response to hypothetical perturbations in vertical profiles of CO_2, H_2O, and aerosols, as well as ground-level O_3. The results, e.g., heating/cooling rates, corresponding to perturbations in O_3 concentrations, were qualitatively compared to some observational data.

In this simple RTM test, the three-dimensional variations in meteorological variables, air pollutant concentrations, and emission rates were ignored. One-dimensional simulations of conditions observed during the primary days of the Portland episode (discussed in Sect. 2.3)

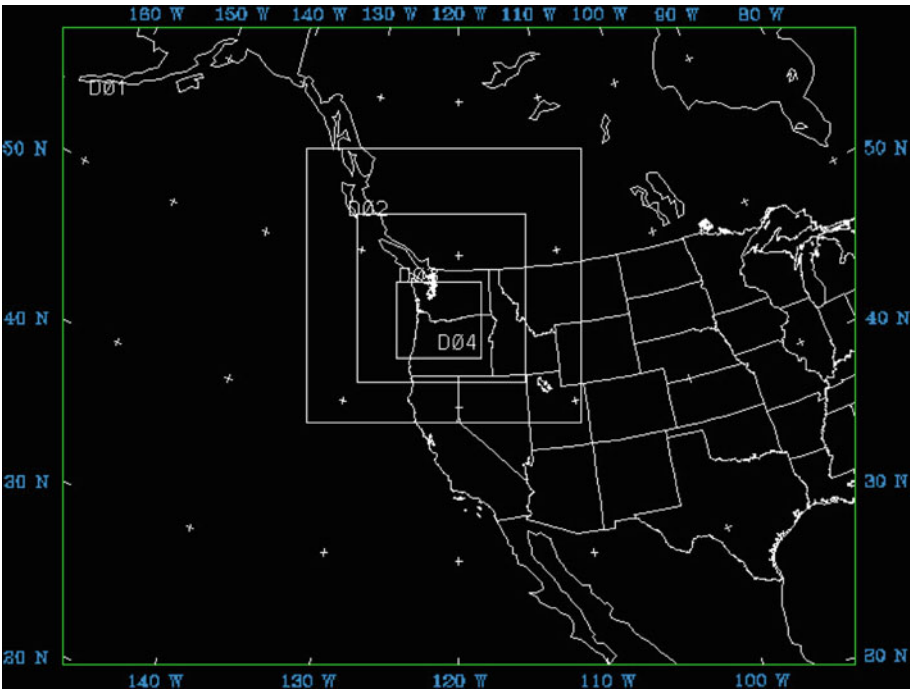

Fig. 2 Meteorological modelling grids for the U.S. Pacific North-West. Domain D04 (4-km grid) is used in the coupled modelling system

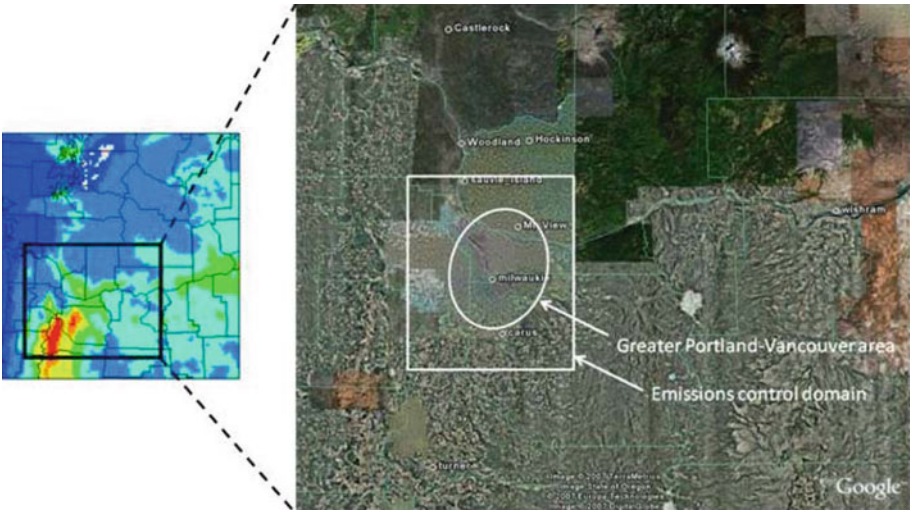

Fig. 3 CMAQ CTM modelling domain (*left*) and detail (*right*), showing the location of the greater Portland-Vancouver urban area (*within the oval*) and an emission control domain (*rectangle*) used in this study. Also shown are locations of some air-quality monitors in the area (Castlerock, Woodland, Hockinson, Sauvie Island, Milwaukie, Carus, Turner, and Wishram)

suggest dependencies of about 0.017 W m^{-2} per ppb O_3. This is comparable with 0.022 W m^{-2} per ppb O_3 that we computed from observational data (IPCC 2001) that correlate changes in mean tropospheric O_3 column with radiative forcing. The RTM test also shows that, for example, a change of 20 ppb in near-surface O_3 imparts a 0.4 W m^{-2} radiative-forcing effect *locally*, which is consistent in order of magnitude with the effects of observed tropospheric ozone enhancements, e.g., as reported by Chan et al. (2001).

This one-dimensional sensitivity analysis also shows that the effects of perturbations in near-surface O_3 are smaller than those of perturbations at higher elevations (up to the tropopause). This is consistent in general with findings from Forster and Shine (1997) showing that a change of 10 Dobson units (DU) of O_3 at 2 km a.g.l. results in a change of 0.025°C in near-surface temperature whereas at about 12 km a.g.l., that same 10 DU perturbation causes a change of 0.175°C in near-surface temperature, i.e., seven times larger.

3.2 Three-Dimensional On-Line Coupled Simulation Results

In this section, we present results from the actual on-line coupled modelling system we described in Sect. 2. First, a meteorological-photochemical base case was established for the Pacific North-West/Portland modelling domain's 4-km grid. The results show that the model captures reasonably well the main features of the O_3 concentrations field during the episode days of interest, including the location of the peaks, 25–75 km south of central Portland, at the Carus and Turner monitors, as observed. However, the model underestimates the peak concentrations, which occur between 1600 and 1800 PDT (PDT: Pacific Daylight Savings Time). Figure 4 depicts the simulated O_3 concentrations field at 1600 PDT (on 26 and 27 July), at the lowest model level, for the base-case scenario and Fig. 5 shows time series of observed and simulated O_3 at two monitor locations (Turner and Wishram). Refer to Fig. 3 for location of monitors.

The CTM's performance was evaluated against EPA-recommended benchmarks for photochemical model skill demonstration (EPA 1999). Here we briefly discuss some aspects of performance for O_3 on days of interest during the episode, focusing on 27July. First, model performance was evaluated in terms of unpaired peak accuracy (*UA*). On 27 July, the observed domain peak (at Carus monitor) was 133 ppb and the simulated peak, without radiative-forcing feedback, was 119.4 ppb ($UA = 0.89$, thus meeting the benchmark of

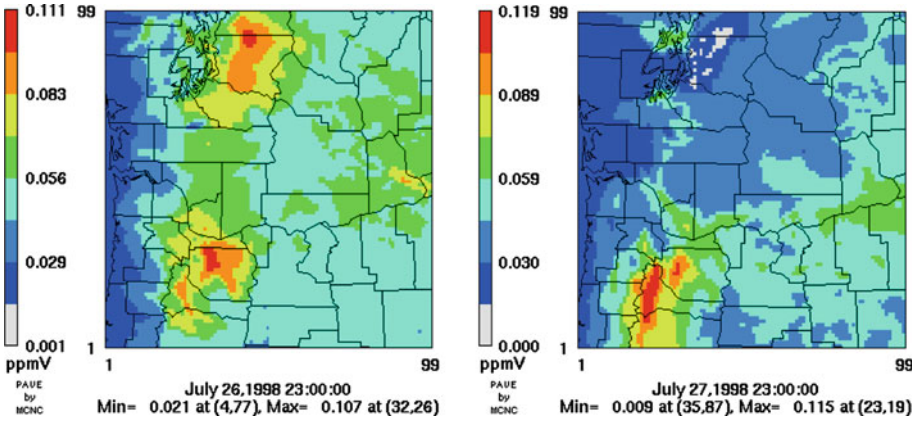

Fig. 4 Base-case O_3 in the 4-km domain: *left*: 26 July at 1600 PDT; *right*: 27 July at 1600 PDT

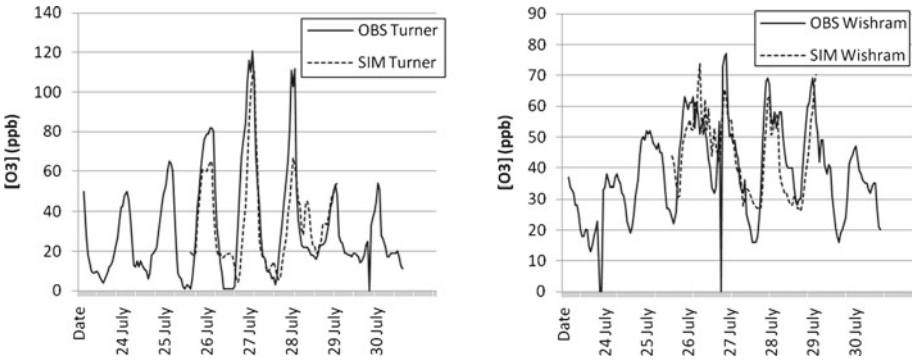

Fig. 5 Observed and simulated O_3 concentrations at two monitors: Turner (*left*) and Wishram (*right*)

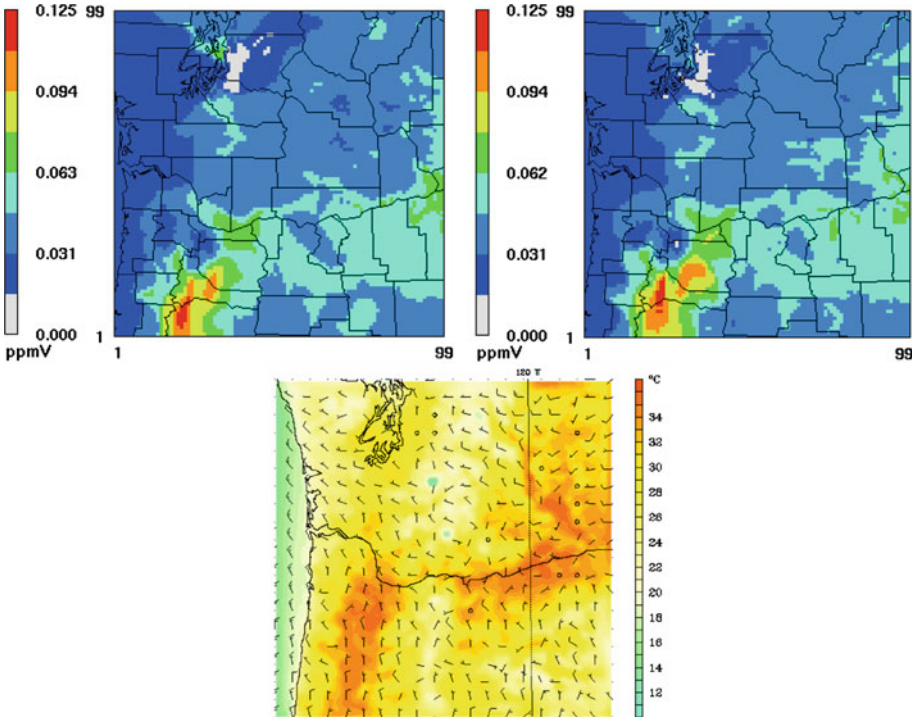

Fig. 6 Base-case O_3 at 1800 PDT on 27 July; *Top left*: without effects of radiative-forcing feedback (peak = 119.4 ppb); *Top right*: with effects of radiative-forcing feedback (peak = 124 ppb). *Bottom*: air temperature (2 m) and wind vector (10 m) fields corresponding to the case with radiative-forcing (i.e., corresponding to the top right figure)

$0.80 \leq UA \leq 1.20$). The inclusion of radiative forcing produced a domain-wide peak of 124 ppb, thus improving *UA* to 0.93, as seen in Fig. 6. The new peak occurs at a slightly different location and the impact of including radiative forcing is not uniform in the domain, i.e., in both the vertical and horizontal directions. There are areas with increase as well as decrease in O_3 (relative to a case without radiative forcing feedback) because of non-linearities in the meteorology-chemistry system.

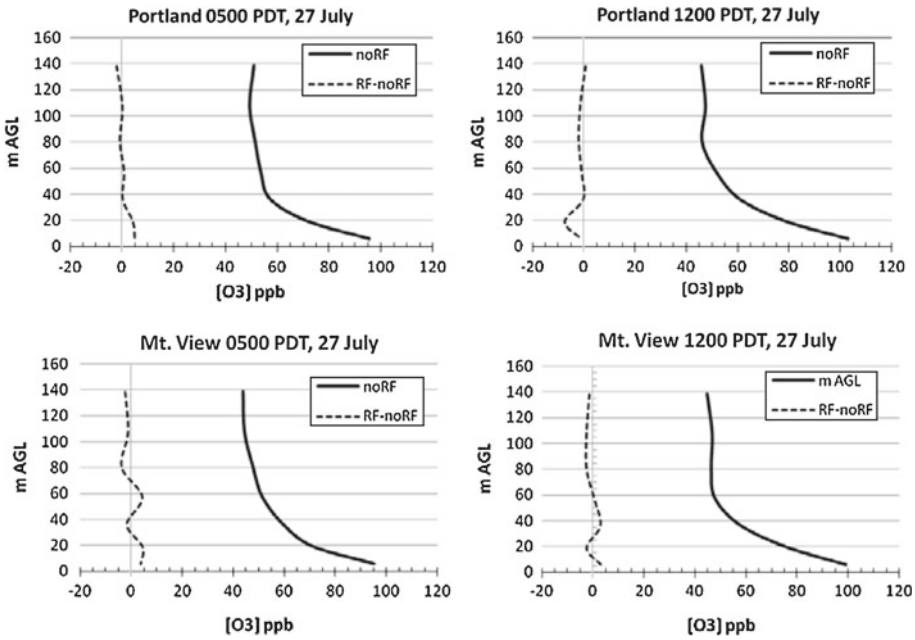

Fig. 7 Vertical profiles of O_3 with and without radiative-forcing feedback at two locations in the Portland urban area. *Solid line* represents absolute values (without radiative-forcing feedback) and the *dashed line* represents departures from that profile for a case with radiative-forcing feedback

Model performance was also evaluated separately at each air-quality monitor (locations shown in Fig. 3). It was found that for observation-simulation data pairs with observed $O_3 \geq 60$ ppb (per EPA model-performance evaluation guidelines), the overall normalized bias (*NB*) was -0.32 and the overall normalized gross error (*NGE*) was 0.33. While the gross error meets the benchmark of $NGE < 0.35$, the bias does not (recommended range for *NB* is to be within ± 0.15) indicating under-prediction of O_3. We also examined the change in model performance, at two monitors closest to urban Portland, after including radiative-forcing feedback. At the Milwaukie monitor, performance was slightly worse after inclusion of radiative forcing (*NB* changed from -0.285 to -0.301 and *NGE* from 0.393 to 0.399) whereas at the Mt. View monitor, performance improved (*NB* changed from -0.253 to -0.227 and *NGE* changed from 0.283 to 0.261).

The vertical profiles of O_3 concentrations were examined for cases with and without radiative-forcing feedback. Figure 7 shows an example at two locations (Downtown Portland, top, and Mt. View, bottom) where the profiles are plotted up to a height of 140 m a.g.l. (roughly the top of the urban canopy layer) for 0500 and 1200 PDT for the base case with and without radiative forcing. Inclusion of radiative forcing resulted in higher O_3 (up to 3.5–4 ppb higher) near the surface and the differences from the case with no radiative forcing (dashed-line profiles) vary with height. In one case (Portland location at 1200 PDT, on 27 July) there is no change near the surface, but a decrease of up to 7 ppb at about 20 m a.g.l. Thus the effect of radiative-forcing inclusion can be different depending on location, vertical level, and time interval.

Another way to evaluate the effects of radiative-forcing feedback on O_3 was to examine the changes averaged over a certain area in the modelling domain. For example, Fig. 8

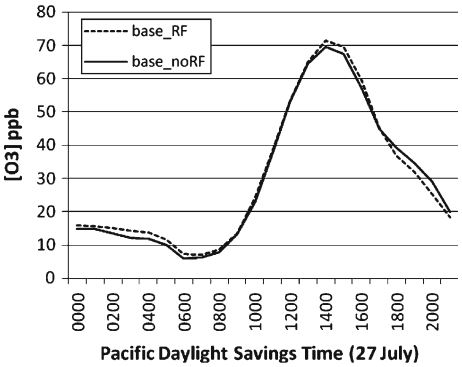

Fig. 8 Area-averaged base-case O_3 (averaged over the urban area) for cases with and without radiative-forcing feedback

Table 1 Simulated domain-wide peak ozone concentrations and impacts of emission control with and without radiative-forcing feedback effects

	Base case peak O_3 (ppb)	Peak after 10% emission reductions (ppb)	Change in peak (ppb)
Without radiative-forcing feedback	119.4	116.1	−3.3
With radiative-forcing feedback (peak paired in time and space)	124.0	119.2	−4.8
With radiative-forcing feedback (peak paired in time only)	124.0	120.6	−3.4

shows the base-case simulated O_3 concentrations with and without radiative forcing (for 27 July) averaged over the urban area shown in Fig. 3 (white rectangle). The inclusion of radiative-forcing feedback imparts an effect of within +2.4 and −3.7 ppb with higher O_3 during nighttime and mid-day hours until about 1700 PDT, after which, O_3 concentrations are lower.

3.3 Emission Control Scenario

As discussed earlier, the simulated domain-wide O_3 peak on 27 July was 119.4 ppb without radiative-forcing feedback. When idealized emission control (a reduction of 10% in anthropogenic emissions) was applied, the new simulated peak was 116.1 ppb, thus a reduction of 3.3 ppb. When the effects of radiative forcing were accounted for, the base-case domain-wide simulated peak became 124.0 ppb and the 10% emission reduction caused this peak (paired in space and time) to decrease to 119.2 ppb, thus a reduction of 4.8 ppb. However, if only pairing in time is considered, that is, at the same time of the base-case peak but at any location, the new peak was 120.6 ppb (which occurred one grid cell away), a reduction of 3.4 ppb. Thus domain-wide, there is a 1.5 ppb effect (reduction in peak) that can be attributed to inclusion of radiative-forcing feedback (if the peak is paired in space and time). If the pairing is in time only, the effect of including radiative-forcing feedback is mostly negligible, i.e., a decrease of 0.1 ppb relative to the case without radiative forcing. Table 1 summarizes these findings.

Table 2 shows another example in evaluating the effects of including radiative forcing, this time for monitor locations at Carus and Turner. The results suggest an additional 1 ppb reduction in the monitor peak that can be attributed to inclusion of radiative forcing feedback.

Table 2 Simulated local ozone peak (at monitor locations) with and without radiative-forcing feedback effects

Monitor location	Change in peak O_3	
	Without radiative-forcing feedback	With radiative-forcing feedback
Carus	−3 (1600 PDT)	−4 (1600 PDT)
Turner	−2 (1700 PDT)	−3 (1700 PDT)

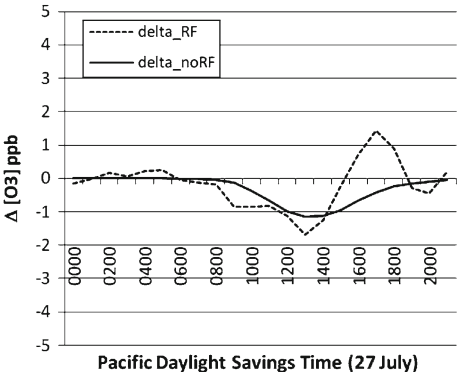

Fig. 9 Area-averaged difference in O_3 resulting from emission reductions (with and without radiative-forcing feedback)

Figure 9 shows changes in O_3 with and without radiative forcing feedback during the hours shown in Fig. 8 and averaged over the urban area shown in Fig. 3. While inclusion of radiative forcing feedback suggests slightly larger decreases in area-averaged midday O_3, e.g., 1.8 ppb versus 1 ppb at 1300 PDT, there also is a negative impact, e.g., an increase of 1.3 ppb at 1700 PDT.

4 Conclusions

We presented an effort to build an on-line coupled meteorology–emissions–chemistry transport modelling system that incorporates feedback from air-quality/chemistry to meteorology. We described an application of the system, as an initial test, in evaluating the effects of changing urban O_3 concentrations on meteorology in the Portland, Oregon area during the episode of 23–31 July 1998.

Results suggest that inclusion of radiative-forcing feedback to meteorology produces small but significant impacts on ozone concentrations. Those impacts become relatively more important when evaluating the effects of emission control strategies. In general, however, we find that inclusion of radiative forcing feedback causes non-directional effects, i.e., both positive and negative, because of the non-linearities involved in the meteorology-chemistry systems.

While we have so far focused only on the radiative forcing effects of ozone, we will update and use the coupled modelling system in the near future in evaluating other effects, including the effects of varying aerosol loading and concentrations of other greenhouse gases. Several related direct and indirect effects of interest will also be evaluated, including any potential impacts from radiative-forcing feedback on cloud fields and, thus, on photochemical production of ozone. The coupled modelling system will be applied to other episodic and seasonal conditions, regions, and a range of emission control scenarios in order to gain a better

understanding of the impacts of radiative forcing on meteorology and air quality under different conditions.

Acknowledgments This material is based upon work supported by the National Science Foundation under Grant No. 0410103. Any opinions, findings, and conclusions or recommendations expressed in this material are those of the authors and do not necessarily reflect the views of the National Science Foundation.

References

Baklanov A, Korsholm U (2007) On-line integrated meteorological and chemical transport modelling: advantages and prospective. In: 29th NATO/SPS international technical meeting on air pollution modeling and its application, 24–28 September 2007, University of Aveiro, Portugal, pp 21–34

Baklanov A, Korsholm U, Mahura A, Petersen C, Gross A (2008) ENVIRO-HIRLAM: on-line coupled modeling of urban meteorology and air pollution. Adv Sci Res 2:41–46

Brieglieb BP, Minnis P, Ramanathan V, Harrison E (1986) Comparison of regional clear-sky albedos inferred from satellite observations and model computations. J Clim Appl Meteorol 25:214–226

Byun D, Schere KL (2006) Review of the governing equations, computational algorithms, and other components of the models-3 Community Multiscale Air Quality (CMAQ) modeling system. Appl Mech Rev 59:51–77

Chan CY, Chan LY, Zheng YG, Harris JM, Oltmans SJ, Christopher S (2001) Effects of 1997 Indonesian forest fires on tropospheric ozone enhancements, radiative forcing, and temperature change over the Hong Kong region. J Geophys Res 106:14875–14885

DEQ (1999) Oregon air quality data summaries. Department of Environmental Quality, State of Oregon, Portland

Dudhia J (1993) A non-hydrostatic version of the Penn State/NCAR mesoscale model: validation tests and simulation of an Atlantic cyclone and cold front. Mon Weather Rev 121:1493–1513

Ebert EE, Curry JA (1992) A parameterization of ice cloud optical properties for climate models. J Geophys Res 97:3831–3836

EPA (1999) Draft guidance on the use of models and other analyses in attainment demonstrations for the 8-hour ozone national ambient air quality standard. Report EPA-454/R-99-004, Office of Air Quality Planning and Standards, U.S. Environmental Protection Agency, Research Triangle Park

Fan H, Sailor DJ (2005) Modeling the impacts of anthropogenic heating on the urban climate of Philadelphia: a comparison of implementations in two PBL schemes. Atmos Environ 39:73–84

Forster PM, Shine KP (1997) Radiative forcing and temperature trends from stratospheric ozone changes. J Geophys Res 102:10841–10855

Fu L, Liou KN (1993) Parameterization of the radiative properties of cirrus clouds. J Atmos Sci 50:2008–2025

Grell GA, Dudhia J, Stauffer DR (1994) A description of the fifth generation Penn State/NCAR mesoscale model (MM5). NCAR Technical Note NCAR/TN—398+STR, National Center for Atmospheric Research, Boulder, 122 pp

Grell GA, Emeis S, Stockwell WR, Schoenemeyer T, Forkel Michalakes RJ, Knoche R, Seidl W (2000) Application of a multiscale, coupled MM5/chemistry model to the complex terrain of the VOTALP valley campaign. Atmos Environ 34:1435–1453

Guenther AB, Zimmerman PR, Harley PC, Monson PK, Fall R (1993) Isoprene and monoterpene emission rate variability—model evaluations and sensitivity analyses. J Geophys Res 98:12609–12617

Hu YX, Stamnes K (1993) An accurate parameterization of the radiative properties of water clouds suitable for use in climate models. J Clim 6:728–742

IPCC (2001) Climate change 2001: the scientific basis. Intergovernmental Panel on Climate Change, Cambridge University Press, Cambridge, 881 pp

Janjic ZI (1994) The step-mountain eta coordinate model: further development of the convection, viscous sublayer, and turbulent closure schemes. Mon Weather Rev 122:927–945

Jin M, Shepherd JM, King MD (2005) Urban aerosols and their variations with clouds and rainfall: a case study for New York and Houston. J Geophys Res. doi:10.1029/2004JD005081

Key J (2001) Streamer user's guide. Cooperative Institute for Meteorological Satellite Studies, University of Wisconsin, Madison

Key J, Schweiger AJ (1998) Tools for atmospheric radiative transfer: streamer and FluxNet. Comput Geosci 24:443–451

Kylling AK, Stamnes K, Tsay S-C (1995) A reliable and efficient two-stream algorithm for spherical radiative transfer: documentation of accuracy in realistic layered media. J Atmos Chem 21:115–150

Naik V, Mauzerall D, Horowitz L, Scharzkopf MD, Ramaswamy V, Oppenheimer M (2005) Net radiative forcing due to changes in regional emissions of tropospheric ozone precursors. J Geophys Res 110:D24306. doi:10.1029/2005JD005908

Pinto JO, Curry JA, Fairall CW (1997) Radiative characteristics of the Arctic atmosphere during spring as inferred from ground-based measurements. J Geophys Res 102:6941–6952

Pleim J, Young J, Wong D, Gilliam R, Otte T, Mathur R (2008) Two-way coupled meteorology and air quality modeling. In: Air pollution modeling and its application, vol XIX. Springer, pp 235–242. doi:10.1007/978-1-4020-8453-9

Schmidt EO, Arduini RF, Wielicki BA, Stone RS, Tsay S-C (1995) Considerations for modeling thin cirrus effects via brightness temperature differences. J Appl Meteorol 34:447–459

Semenza JC, Wilson DJ, Parra J, Bontempo B, Hart M, Sailor DJ, George LA (2008) Public perception and behavior change in relationship to hot weather and air pollution. Environ Res 107:401–411

Snell HE, Anderson GP, Wang J, Moncet J-L, Chetwybd JH, English SJ (1995) Validation of FASE and MODTRAN3: updates and comparisons with clear-sky measurements. In: SPIE conference 2578, Paris, France, 1995, pp 194–204

Stamnes K, Tsay S-C, Wiscombe W, Jayaweera K (1988) Numerically stable algorithm for discrete-ordinate-method radiative transfer in multiple scattering and emitting layered media. Appl Opt 27:2502–2509

Taha H (2008a) Meso-urban meteorological and photochemical modeling of heat island mitigation. Atmos Environ 42:8795–8809. doi:10.1016/j.atmosenv.2008.06.036

Taha H (2008b) Episodic performance and sensitivity of the urbanized MM5 (uMM5) to perturbations in surface properties in Houston TX. Boundary-Layer Meteorol 127:193–218. doi:10.1007/s10546-007-9258-6

Takano Y, Liou KN (1989) Solar radiative transfer in cirrus clouds. Part I: Single-scattering and optical properties of hexagonal crystals. J Atmos Sci 46:3–19

Toon OB, McKay CP, Ackerman TP (1989) Rapid calculations of radiative heating rates and photodissociation rates in inhomogeneous multiple scattering atmospheres. J Geophys Res 94:16287–16301

Tsay S-C, Stamnes K, Jayaweera K (1989) Radiative energy budget in the cloudy and hazy Arctic. J Atmos Sci 46:1002–1018

WMO (2008) Joint report of COST action 728 and GURME: overview of existing integrated (off-line and on-line) mesoscale meteorological and chemical transport modeling systems in Europe. World Meteorological Organization, Geneva